Analysis of the Vertebral Morphology of Pacific Sand Lance, *Ammodytes personatus*

Elynore S. In[1], Owen M. Proulx[1], Tatiana N. Egbert[2], Cassandra M. Donatelli[3], Karly E. Cohen[4]

1: Department of Marine Biology, College of the Environment, University of Washington, Seattle, WA 98195

2: Department of Biology, School of Science, Technology, Engineering and Mathematics, University of Washington, Bothell, WA 98011

3: School of Engineering and Technology, University of Washington, Tacoma, WA 98402

4: University of Washington, Friday Harbor Laboratories, Friday Harbor, WA 98250

Keywords: vertebral morphology, functional morphology, *Ammodytes personatus,* CT scanning

Abstract

Pacific sand lance (*Ammodytes personatus)* are small head-first burrowing fish distributed throughout the North Pacific Ocean. Despite lacking typical morphology of other burrowers, their elongate bodies allow for rapid burrowing through undulation. Vertebrae support full-body movements like swimming and bear the mechanical load for the axial skeleton. We hypothesize that structural changes in vertebrae, such as changes in mineralization and shape, enhance undulatory performance and help generate the forces needed for burial. We microCT scanned 22 sand lance (SL 33-95mm) to estimate the bone mineral density and used geometric morphometrics to characterize shape variation along the length of the fish and over ontogeny. We found sand lance vertebrae were 1.25 times denser near the head and tail regions compared to the middle. Additionally, the main drivers of vertebral shape variation were the prominence of the hemal spine and the angle of the neural and hemal spines relative to the centrum. These localized morphological increases in density and shifts in spine orientation may serve as additional support and points of force transmission for initiating and sustaining burial.

Introduction

Burrowing, movement through soft substrate or material, is a widespread behavior observed across diverse animal taxa, from invertebrates to vertebrates, serving various ecological functions such as predator avoidance, habitat construction, and thermoregulation. The capacity for burrowing is determined by a combination of morphological and physiological traits, which are often tied to the environment of the burrowing organism as well as the burrowing mechanism.

The morphology found in burrowing animals varies greatly. For example, the European mole (*Talpa europaea*) relies on reinforced forelimbs and large claws to displace compacted soil (Gambaryan et al, 2002). Ghost crabs (*Ocypode quadrata*) employ rapid, coordinated digging motions utilizing back legs and unequally-sized front claws to carve out burrows in sandy environments (Chan et al., 2006). In some terrestrial insects, such as the neotropical millipede (*Nyssodesmus pythonmillipedes*), calcified exoskeletons may also contribute to burrowing locomotion by resisting the large crushing forces generated in the process (Borrell, 2004). The mechanical support provided by mineralization in these structures serves to increase the stiffness of the body as millipedes break through dense soils. These distinct but functionally analogous approaches highlight how morphology in burrowing species is shaped by both the mechanical constraints of burrowing methods and ecological pressures.

Burrowing in aquatic environments imposes a distinct set of biomechanical challenges compared to terrestrial settings. Organisms must navigate shifting sediments, resist hydrodynamic forces, and penetrate through substrates where grain size, compaction, and cohesion can vary dramatically (Dorgan et al., 2006). Many aquatic burrowers rely on sediment fluidization to reduce the substrate resistance, using behavior and morphological strategies to transiently alter the mechanical state of the sediment (Dorgan, 2015). Some bivalves (*Ensis spp.)* use a dual anchor system to close valves and force fluid from the pericardial cavity into the foot, using the foot as an anchor. At the same time, water from the mantle cavity liquefies the sand around the shell, facilitating movement (Dorgan, 2015; Trueman, 1996). The effectiveness of these burrowing techniques depends heavily on the properties of the substrate, such as grain size and

compaction, which influence the energy required to penetrate and maintain a burrow. In sandy marine environments, organisms experience selective pressures related to substrate instability and hydrodynamic forces. For example, some wrasses of the family *Labridae* exhibit sand-diving behavior by quickly and forcefully penetrating the substrate surface, and subsequently undulating from head to tail (Tatom-Naecker T-AM, Westneat MW, 2018). Sand-diving in wrasses is a burrowing strategy thought to aid the fish's initial penetration of the sand as it acts as a solid, while undulation beneath the surface is employed as sand acts more like a fluid. It is also known that the skull morphology of sand-diving wrasses include slender, elongate shapes as well as blunt, laterally compressed shapes which may both enable their head-first sand-diving behavior.

As seen in the case of the neotropical millipede, adaptations to morphology such as increased mineralization in the head or tail or unique body shapes, are critical for sustaining movement through dense underground substrates. This same principle applies in aquatic environments. The rice paddy eel (Pisodonophis boro), for instance, demonstrates dual burrowing modes—head-first and tail-first—each supported by a suite of adaptations. A heavily ossified skull, robust premaxilla, and reduced eyes facilitate head-first entry, while tail-first burrowing is enabled by fused caudal vertebrae, the absence of a caudal fin, and a hardened, tapered tail (De Schepper et al., 2007).

Burrowing, while often supported by morphological adaptations of limbs or skulls, can also be enabled by the trunk of the body. For example, the Australian salamanderfish *Lepidogalaxias salamandroides* has a wedge-shaped skull, widely spaced vertebrae, and long, slender ribs which improve the flexibility of the spinal column, allowing for s-shaped body movements for burrowing through moist sand (Berra and

Allen, 2011). Similarly, sand lances, members of the family *Ammodytes,* employ below-ground undulation to aid their burrowing, but lack typical morphological adaptations seen in other burrowing fish and the anatomical modifications of the skeleton that contribute to burrowing behavior remain unclear.

The Pacific sand lance (*Ammodytes personatus*) is a small, elongate forage fish widely distributed in the North Pacific Ocean. They play a crucial role in marine ecosystems as a primary prey source for seabirds, marine mammals, and commercially valuable fish species throughout different stages in their life history, providing a link between primary and secondary producers to upper trophic level species (Bizzarro, et al., 2016). Sand lance exhibit a unique life history strategy that involves rapidly burrowing into sandy substrates to avoid predation as well as entering a state of dormancy underground during winter months (Staudinger et al., 2020). Juvenile sand lance remain pelagic until they reach approximately 35–50 mm SL, at which point they transition to a benthic burrowing lifestyle (Bizzarro et al., 2016).

While *A. personatus* has an elongate body shape, the complex skull morphology and prominent eyes set this species apart from other burrowing fish (Bizzarro et al., 2016). Additionally, no sediment fluidization behavior is observed in *A. personatus.* Instead, the fish is initially propelled by undulatory movements of the tail until the below-ground anterior portion of the body takes over (Gidmark et al., 2011). This prompts an investigation into the morphology of *A. personatus* vertebrae, which provides the base for full body movements like undulation and bears the mechanical burden for the axial skeleton. By analyzing the patterns of vertebral mineralization and morphological

variation, we hope to better understand the skeletal modifications that enable efficient burrowing in *A. personatus*.

Mineralization of skeletal structures plays a critical role in determining biomechanical performance, particularly in species that rely on skeletal reinforcement for movement and substrate interaction such as *A. personatus*. Traditional methods for measuring skeletal density include ashing techniques and microhardness testing (Currey, 1984). However, advancements in imaging technology have led to the widespread use of micro-computed tomography (μCT) scanning, which allows for non-destructive, high-resolution analysis of skeletal structures, particularly useful for small anatomy such as vertebrae (Buser et al., 2020). μCT scanning provides detailed three-dimensional reconstructions of mineralized tissues, making it an ideal method for assessing skeletal adaptations in burrowing organisms.

The goal of this study is to quantify how mineralization patterns in *A. personatus* vertebrae vary across skeletal regions and ontogenetic stages, and to assess whether these patterns contribute to burrowing performance. Specifically, we (1) quantified vertebral mineral density across different skeletal regions over ontogeny, (2) characterized and quantified vertebral shape variation, and (3) evaluated the functional implications of mineral distribution and morphology for burrowing. By integrating μCT scanning techniques with morphological analysis, this study provides new insights into skeletal adaptations that facilitate burrowing in *A. personatus*.

Methods

CT Scanning

We µCT scanned *Ammodytes personatus* (Pacific Sand Lance, $n = 22$), specimens ranging from 33 mm to 95 mm in standard length (SL). All samples were collected from the waters surrounding Friday Harbor, WA, using seine netting in accordance with IACUC protocol number 026. Each specimen was scanned in a vertically upright position and stabilized with foam. Two hydroxyapatite phantoms of 25% and 75% density were included in every scan. Hydroxyapatite is the mineral found in bone and allows us to have a reference of known density to compare our sand lance bone density to and standardize our CT scan data. All samples were scanned using a Bruker SkyScan 1273 and reconstructed using NRECON (Micro Phonotics Inc., Allentown, PA., USA), and rendered in 3D Slicer (slicer.org) using the SlicerMorph Module (developed by Murat Maga, SCRI.).

Table 1: CT metadata for Sand lance specimens used in this study.

Genus	Species	Location Collected	Location Scanned	Standard Length (mm)	Resolution (µm)	Exposure (ms)	Voltage (kV)	Current (µA)
Ammodytes	*personatus*	Friday Harbor, WA	Karel F. Liem Bioimaging Center	34	10	240	40	160
Ammodytes	*personatus*	Friday Harbor, WA	Karel F. Liem Bioimaging Center	34	10	240	40	160
Ammodytes	*personatus*	Friday Harbor, WA	Karel F. Liem Bioimaging Center	40	10	240	40	160
Ammodytes	*personatus*	Friday Harbor, WA	Karel F. Liem Bioimaging Center	33	13	202	50	160
Ammodytes	*personatus*	Friday Harbor, WA	Karel F. Liem Bioimaging Center	35	13	202	50	160
Ammodytes	*personatus*	Friday Harbor, WA	Karel F. Liem Bioimaging Center	58	18	99	100	150
Ammodytes	*personatus*	Friday Harbor, WA	Karel F. Liem Bioimaging Center	59	18	99	100	150
Ammodytes	*personatus*	Friday Harbor, WA	Karel F. Liem Bioimaging Center	50	20	102	50	300
Ammodytes	*personatus*	Friday Harbor, WA	Karel F. Liem Bioimaging Center	50	20	102	50	300
Ammodytes	*personatus*	Friday Harbor, WA	Karel F. Liem Bioimaging Center	65	20	157	50	200
Ammodytes	*personatus*	Friday Harbor, WA	Karel F. Liem Bioimaging Center	70	20	157	50	200

Ammodytes	*personatus*	Friday Harbor, WA	Karel F. Liem Bioimaging Center	55	22	108	90	166
Ammodytes	*personatus*	Friday Harbor, WA	Karel F. Liem Bioimaging Center	59.2	22	108	90	166
Ammodytes	*personatus*	Friday Harbor, WA	Karel F. Liem Bioimaging Center	65.1	22	108	90	166
Ammodytes	*personatus*	Friday Harbor, WA	Karel F. Liem Bioimaging Center	91	22	108	90	166
Ammodytes	*personatus*	Friday Harbor, WA	Karel F. Liem Bioimaging Center	68	35	57	70	300
Ammodytes	*personatus*	Friday Harbor, WA	Karel F. Liem Bioimaging Center	72.5	35	57	70	300
Ammodytes	*personatus*	Friday Harbor, WA	Karel F. Liem Bioimaging Center	75	35	57	70	300
Ammodytes	*personatus*	Friday Harbor, WA	Karel F. Liem Bioimaging Center	75	35	57	70	300
Ammodytes	*personatus*	Friday Harbor, WA	Karel F. Liem Bioimaging Center	95	37	57	70	300
Ammodytes	*personatus*	Friday Harbor, WA	Karel F. Liem Bioimaging Center	66	40	57	70	300
Ammodytes	*personatus*	Friday Harbor, WA	Karel F. Liem Bioimaging Center	66	40	57	70	300

Bone mineral density (BMD) calculations

We digitally segmented 330 vertebrae from three different regions along the spine: the anterior, middle, and caudal regions. The anterior region was defined as the five vertebrae closest to the head, excluding the first two atlas vertebrae. The middle region consisted of five vertebrae located centrally within the fish, selected as half way between the head and the tail based on the fish's standard length. Finally, the caudal region was designated as the last five vertebrae at the rear of the fish, excluding the two vertebrae closest to the tail.

Brightness in CT scans correlates to density (and therefore mineralization), with brighter regions being more dense and darker regions less dense. Each segment of 5 vertebrae from the anterior, middle, and caudal regions of each fish was analyzed through the Segment Statistics module (*Andras Lasso (PerkLab), Christian Bauer (University of Iowa), Steve Pieper (Isomics)*) in 3D Slicer, and the average voxel brightness for each

region was documented. The hydroxyapatite phantoms were segmented by analyzing a region inside each one devoid of empty space; this gave us the average voxel brightness of objects of known densities. As multiple sand lance are present in each scan, the average voxel brightness of the phantoms could be reused in mineralization analysis for each fish within the phantoms corresponding scan. As the density of hydroxyapatite for each phantom is known (25% and 75%), we compared the average voxel brightness of the phantoms to the average voxel brightness of the vertebrae segments (anterior, middle, and caudal) of each fish to determine the density, or mineralization, of each region. Bone mineral density (BMD) was calculated using the equations:

$$Slope = \frac{(75-25)}{\frac{(Mean\ Brightness\ of\ 75\%\ phantom)}{(Mean\ Brightness\ of\ 25\%\ phantom)}}$$

$$Intercept = 25 - Mean\ of\ 25\% * Slope$$

$$BMD = Slope * Mean\ of\ Vertebrae + Intercept$$

Geometric Morphometrics

Variation in the shape of morphological structures can also be characterized through geometric morphometrics, a powerful tool which analyzes Cartesian coordinates of anatomical landmarks using multivariate statistics (D. E. Slice, 2007). Geometric morphometrics can be used directly on μCT scans by manually or automatically placing landmarks on homologous anatomical features of multiple specimens, capturing minute differences in structures and providing a quantitative analysis of the drivers of variation.

A subset of 11 individuals were used to perform geometric morphometric analysis, and each fish had 5 vertebrae that were chosen for landmarking. A total of 12

landmarks per vertebrae were selected to characterize the major anatomy of each vertebrae, consistent in placement and order among the total 60 vertebrae. These landmarks were placed on the tip of the neural spine, the two zygapophoses, around the centrum, and on the tip of the hemal spine (Figure 1). For vertebrae lacking hemal spines, analogous landmarks were placed where the spines begin to protrude (parapophyses or hemapophyses). These points were chosen for their ability to clearly define the overall shape of a vertebra, as well as provide measurements of key angles, such as between the neural spine and top of the centrum. Landmarks were placed in 3D Slicer using the 'Markups' module, and exported into R for statistical analysis.

Geometric morphometrics analysis was performed using the package geomorph v4.0 (Adams D, Collyer M, Kaliontzopoulou A, Baken E, 2025). Generalized Procrustes Analysis (GPA) was performed to superimpose the coordinates of landmarks using the function *gpagen*. Principal component analysis (PCA) was subsequently used to determine the main axes of variation in shape in the dataset, using the function *gm.prcomp*. To calculate the predicted mean shape of principal component extremes, the function *mshape* was used.

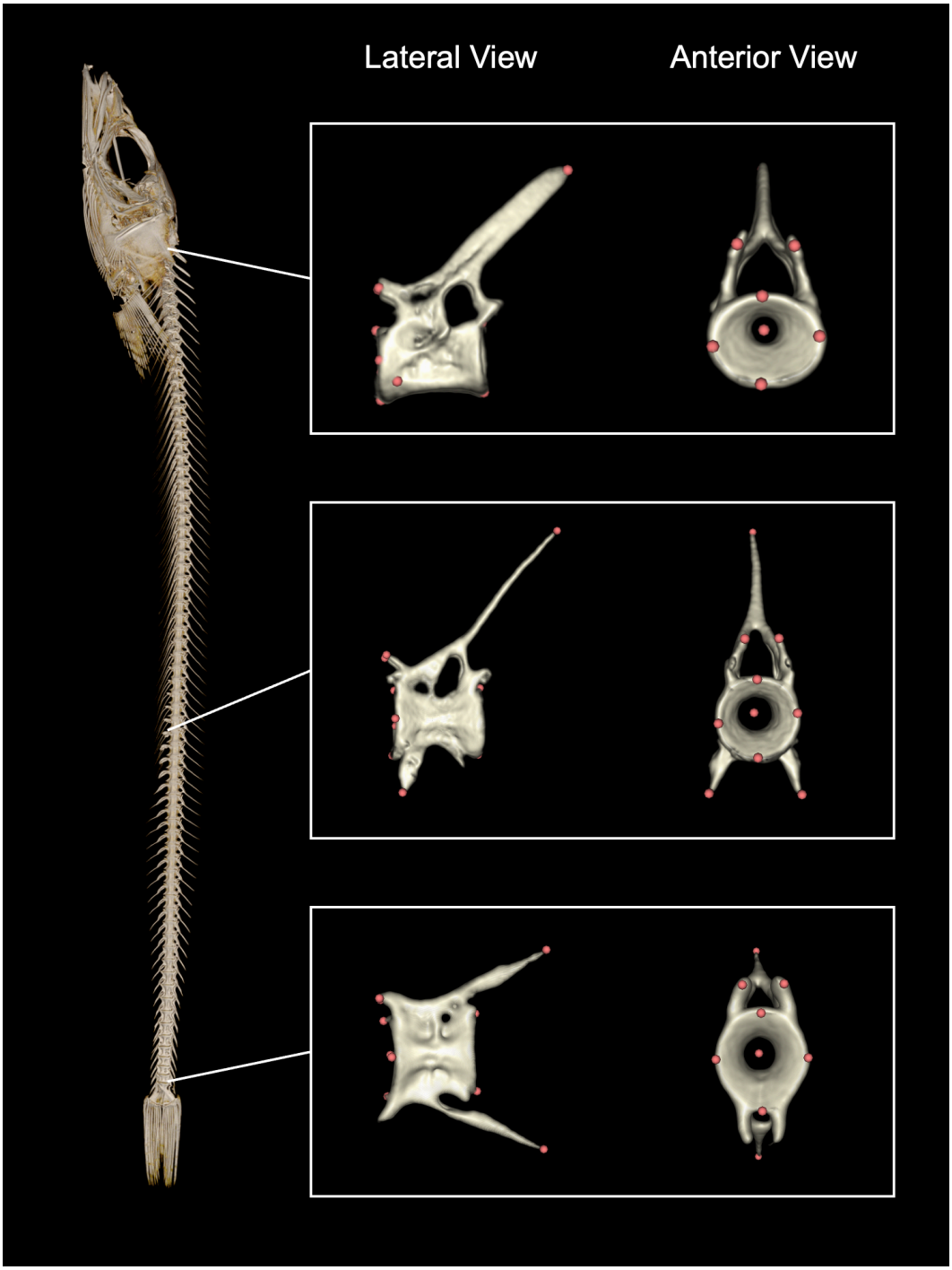

Figure 1. Three-dimensional scheme for placement of landmarks for analysis of vertebrae from the postcranial region (top row), middle region (second row), and caudal region (bottom row).

Statistics

All mineralization statistical analyses were done using R Version 4.3.2 with the packages dplyr (Wickham H, François R, Henry L, Müller K, Vaughan D, 2023), readxl, stringr (Wickham, 2023), and plotted using ggplot2 (H. Wickham, 2016), RColorBrewer (Neuwirth, 2022), cowplot (Wilke, 2024), and ggpubr (Kassambara, 2023). Analysis of variance (ANOVA) tests and t-tests were used to determine statistical differences between mean bone mineral density for distinct vertebral regions and over ontogeny.

Results

Bone mineral density (BMD)

Between the anterior, middle, and caudal regions of the vertebral column, the percentage of hydroxyapatite was not significantly different for the anterior and caudal regions ($p=0.49$), however the middle region was significantly different to both the anterior and caudal (Figure 2). The mean bone mineral density for the anterior vertebrae was 44.96% Hydroxyapatite (HxA) (SD =9.81), 35.92% HxA for the middle (SD=6.28), and 45.83% HxA for the caudal region (SD=8.96). Anterior vertebrae were more mineralized than middle vertebrae ($p < 0.0001$) by approximately 25%, and caudal vertebrae were more mineralized than middle vertebrae ($p < 0.0001$) by approximately 27.5%.

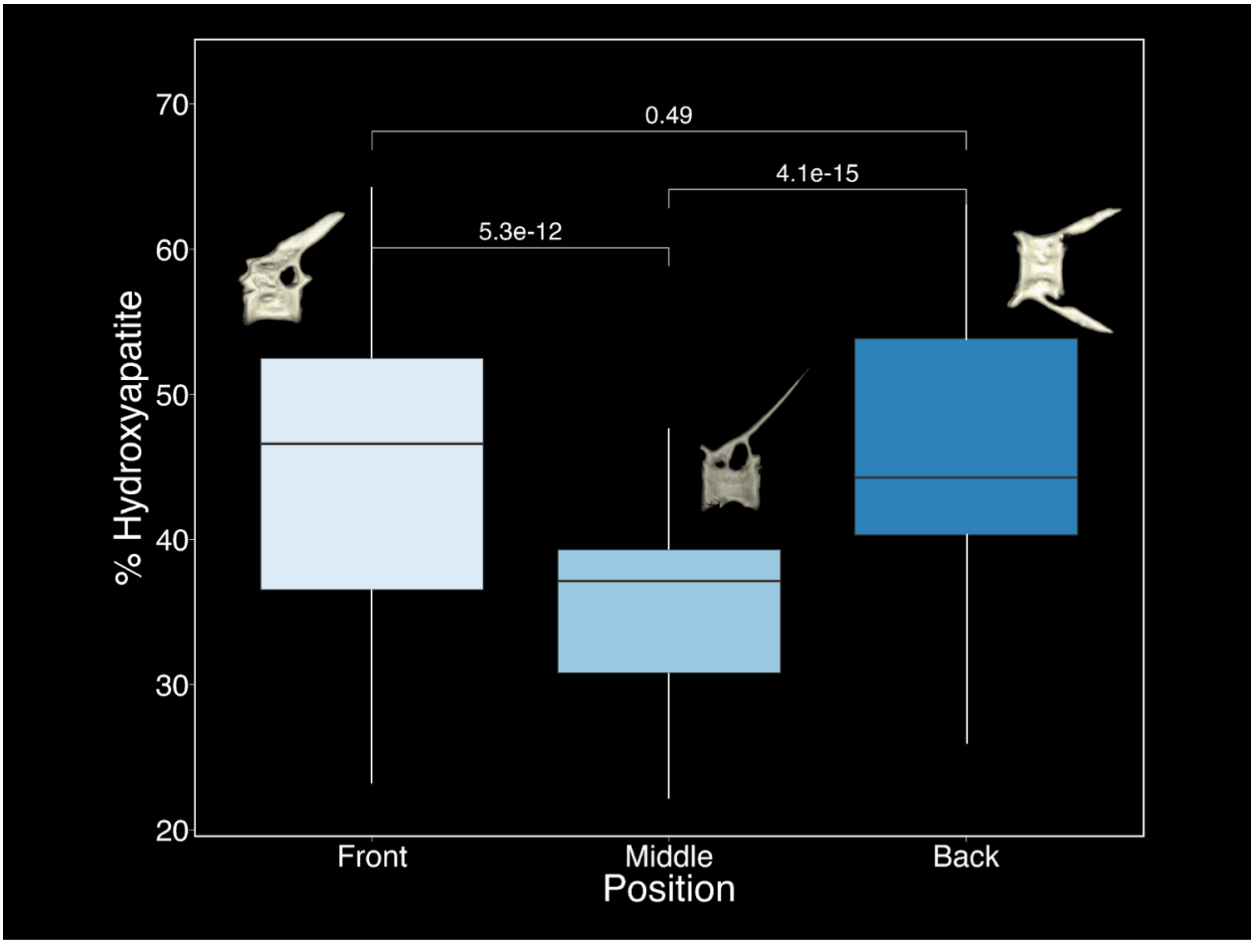

Figure 2. Boxplot showing the percentage of hydroxyapatite in vertebrae across three regions of the vertebral column: anterior, middle, and caudal. Statistical comparisons indicate that the anterior vertebrae had significantly higher mineralization than the middle vertebrae ($p = 5.2e-12$), and the caudal vertebrae had significantly higher mineralization than the middle vertebrae ($p < 4.1e-15$), but the anterior and caudal regions were not statistically different from each other ($p=0.49$).

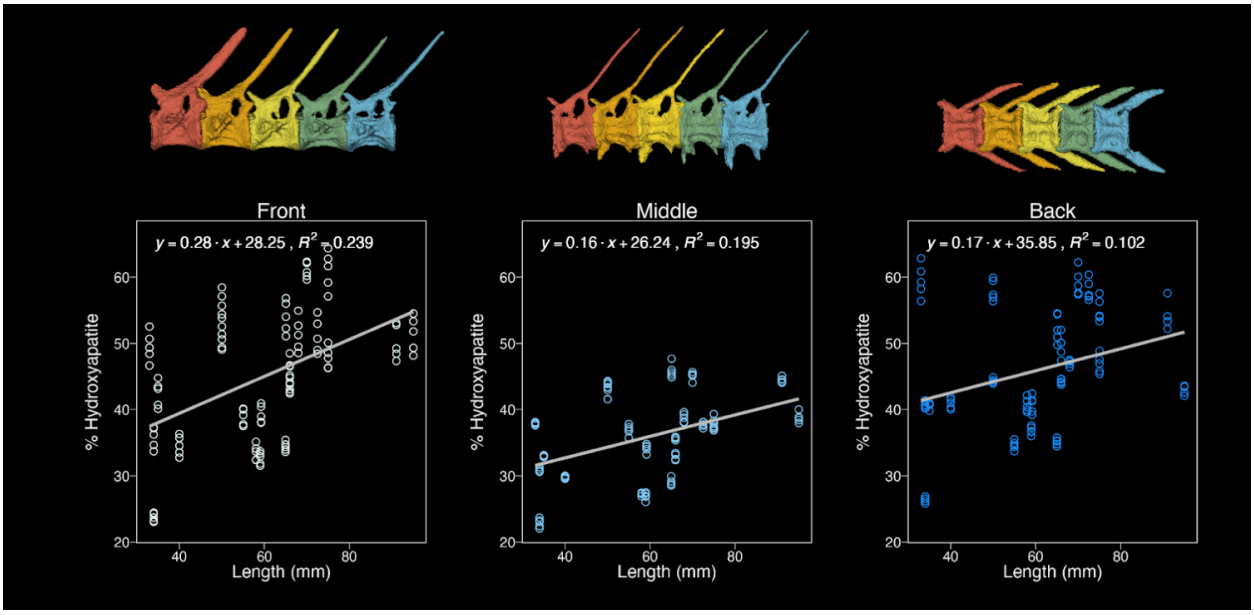

Figure 3. Scatter plots showing the relationship between fish length (mm) and the percentage of hydroxyapatite in vertebrae at three positions: anterior, middle, and caudal. Each point represents a single vertebra. A weak positive correlation was observed in all regions, with the anterior vertebrae exhibiting the strongest relationship ($R^2 = 0.239$), followed by the middle ($R^2 = 0.195$) and caudal ($R^2 = 0.102$). These results suggest a minor trend of increased vertebral mineralization with fish length. Above the graph are example segments of vertebrae from each region for reference.

For each position in the vertebral column, there is a weak positive relationship between length of the fish and the percentage of hydroxyapatite in their vertebrae (Figure 3). One point represents a single vertebrae. This suggests that as sand lance get older, the mineralization of their vertebrae increases. The anterior vertebrae had the strongest correlation ($R^2 = 0.239$) compared to the middle ($R^2 = 0.195$) and caudal ($R^2 = 0.102$), however, because these R^2 values are quite low, the length of the fish alone does not fully explain the variation in mineralization. This could be due to other factors that were not measured, such as behavior, diet, or habitat.

ANOVA tests comparing position and length with BMD suggest that both are significant predictors of bone mineral density ($p < 0.0001$ for both), and both fish length and vertebral position significantly affect mineralization.

Pairwise t-tests using pooled standard deviation between the vertebral positions suggest the differences between the bone mineral density for anterior and caudal vertebrae were not significant ($p=1.0$). However, the p-value for the comparison between the anterior and middle vertebrae as well as middle and caudal vertebrae was significant ($p < 0.0001$ for both).

Geometric Morphometrics

Figure 4. 3D rendered microCT scans of vertebrae across the length of a sand lance. (SL=58mm)

Our PCA results suggest the main axis of shape variation (PC1) is related to the absence or presence of the hemal spine of the vertebrae and the relative position of the neural spine. The extremes of this axis are grouped into specific clusters by vertebral position (Figure 5). Vertebra 1, 2, and 3, which are closest to the anterior region, lack hemal spines and instead are attached to ribs. Vertebra 4 and 5 have well developed hemal spines. Shape changes on the PC2 axis correspond to the angle made by the neural spine and the hemal spine connecting at the centrum. Vertebrae on the minimum extreme

exhibit more vertical, obtuse angles, while the maximum extreme exhibits steeper, more acute angles. On the third PC axis, shape changes coincide with SL of sand lances, suggesting a change over ontogeny. On this axis, the minimum extreme mean shape has a wider centrum and shorter neural spine, while the maximum extreme has a narrow centrum and elongated neural spine.

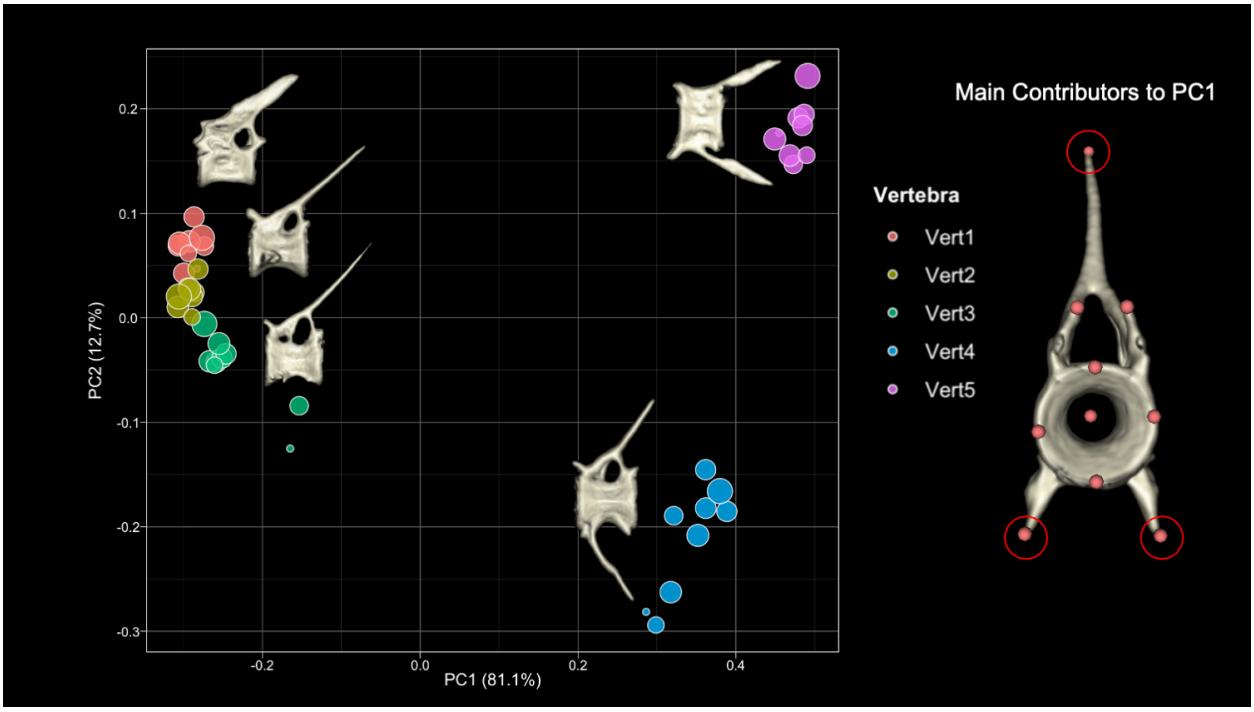

Figure 5. Principal component analysis results of individual landmarks' contribution to variation, plotting PC1 on the x-axis (81.1% of the variation) and PC2 on the y-axis (12.7% of the variation). One dot represents one vertebrae; the

size of the dot corresponds to the relative standard length of the fish.f

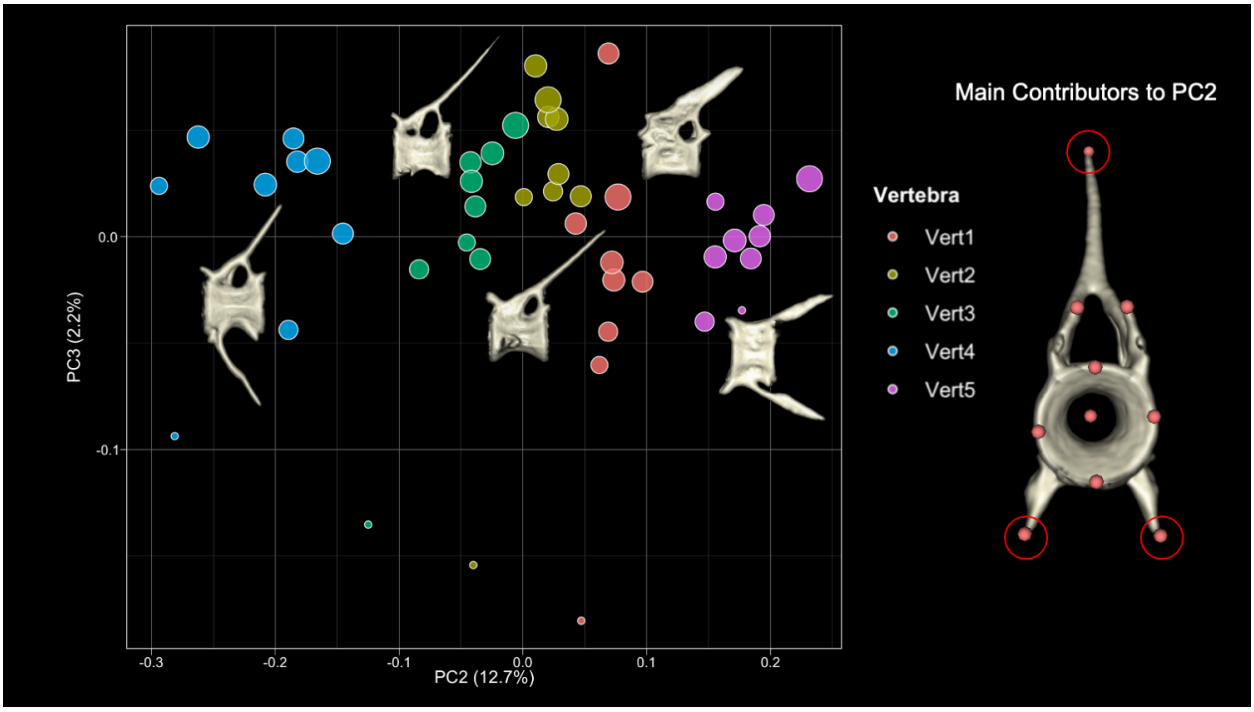

Figure 6. Principal component analysis results of individual landmarks' contribution to variation, plotting PC2 on the x-axis (12.7% of the variation) and PC3 on the y-axis (2.2% of the variation).

Discussion

In a head-first burrowing fish species, we find evidence that the vertebral morphology of *Ammodytes personatus* serves a functional purpose related to the burrowing behavior of this fish, especially in the caudal region. The vertebral mineralization pattern and shape changes in *A. personatus* reflects the need for a balance between flexibility and stiffness, and ontogenetic changes suggesting that skeletal development is influenced by both mechanical demands and the life history of the fish. Mineralization of the caudal and post-cranial vertebrae were significantly different from the middle vertebrae as they exhibit higher percentage of hydroxyapatite, suggesting regional differences in skeletal stiffness. Additionally, the main axes of vertebral shape

variation were related to the presence of hemal spines, the angle between neural and hemal spines, and the width of the centra over ontogeny, which coupled with mineralization data, emphasize the role of the tail vertebrae in undulation.

The possession of the hemal spine in the caudal region suggests a purpose to protect the caudal artery and vein (Galbusera and Bassani, 2019) but also provide the structure for the generation of thrust. Vertebrae located in the trunk region of the sand lance lack the fusion of the parapophyses into the hemal spine, instead connecting to the rib projections that surround the abdominal cavity. A large quantity of vertebrae with hemal spines (over 50%) suggest that *A. personatus* have a need for speed: the tail must generate high forces and amplitudes to be able to burrow and swim. Additionally, we observed that the angle of the hemal and neural spines relative to the centrum varies. As neural and hemal spines serve as the attachment point for collagen and muscle fibers throughout the body (Westneat & Wainwright, 2001), steeply angled neural and hemal spines in the anterior and posterior vertebrae allow the vertebrae to be the anchor for the immense forces generated during swimming and burrowing, underscoring the role of the vertebrae near the tail.

High values of mineralization correlate with low measures of elasticity, or high values of stiffness (Currey, 1984). In studies that compared the undulatory swimming of biomimetic models of different fish species, body stiffness is suggested as a key parameter that governs locomotion (Shelton et al., 2014). The middle region having the lowest mineral content may allow for greater flexibility. As sand lance utilize undulation for swimming and burrowing, having a flexible region in the middle may increase the amplitude of their undulations and increase their swimming speed or burial efficiency.

The burial behavior of *A. personatus* has three stages: 1) undulations that push the head into the sand, 2) more pronounced undulations that push the rest of the body into the sand, and 3) subterranean undulation while the tail above ground stops generating motion (Gidmark et al., 2011). It is possible that as the length of the fish increases over ontogeny, more mineralized and more rigid caudal vertebrae coupled with the flexible middle region could help produce the force needed to aid rapid burial.

Vertebral mineralization correlates weakly yet positively with total fish length suggesting that ontogenetic changes in skeletal composition are at play, albeit influenced by factors beyond size alone. In some species within the Liparidae family, bone mineral density variation seems to be related to multiple environmental factors, including habitat and depth. Polar and pelagic snailfish species have less dense bones than demersal species, which could be driven by a need for maintaining buoyancy (Gerringer et al., 2021). Although *A. personatus* is a shallow-water species, this example highlights the plasticity of skeletal mineralization in response to ecological pressures.

Our findings indicate that bone mineral density in anterior and middle vertebrae is significantly correlated with body length, suggesting a growth-related increase in mineralization. In contrast, caudal vertebrae appear to require a specific level of mineral density, potentially due to functional demands such as swimming or burrowing. The progressive increase in BMD in the anterior and middle vertebrae as fish grow might be necessary to provide the structural support required for effective burrowing. Additionally, juveniles sand lances were observed to have wider centra and shorter neural spines compared to adults. This could suggest a selective pressure for mineral sequestration as juveniles must burrow during their first winter.

Overall, we find that the mineralization and shape of vertebrae near the head and tail are structurally adapted for fast, efficient undulatory movement while the trunk vertebrae may be more appropriate for flexibility, both types of movement that are necessary for burrowing. The size and shape changes of vertebrae of smaller juveniles compared to adults also has implications for the evolutionary pressures of juveniles who begin burrowing within their early years of life.

References

Adams D, Collyer M, Kaliontzopoulou A, Baken E (2025). "Geomorph: Software for geometric morphometric analyses. R package version 4.0.10." <https://cran.r-project.org/package=geomorph>.

Baken E, Collyer M, Kaliontzopoulou A, Adams D (2021). "geomorph v4.0 and gmShiny: enhanced analytics and a new graphical interface for a comprehensive morphometric experience." *Methods in Ecology and Evolution*, **12**, 2355-2363.

Berra, T. M., & Allen, G. R. (1989). Burrowing, Emergence, Behavior, and Functional Morphology of the Australian Salamanderfish, *Lepidogalaxias salamandroides*. *Fisheries*, *14*(5), 2–10. https://doi.org/10.1577/1548-8446(1989)014%253C0002:BEBAFM%253E2.0.CO;2

Bizzarro, J. J., Peterson, A. N., Blaine, J. M., Balaban, J. P., Greene, H. G., & Summers, A. P. (2016). Burrowing behavior, habitat, and functional morphology of the Pacific sand lance (Ammodytes personatus). *Fishery Bulletin*, *114*(4), 445–460. https://doi.org/10.7755/FB.114.4.7

Borrell, B. J. (2004). Mechanical properties of calcified exoskeleton from the neotropical millipede, Nyssodesmus python. *Journal of Insect Physiology*, *50*(12), 1121–1126. https://doi.org/10.1016/j.jinsphys.2004.09.012

Buser, T. J., Boyd, O. F., Cortés, Á., Donatelli, C. M., Kolmann, M. A., Luparell, J. L., Pfeiffenberger, J. A., Sidlauskas, B. L., & Summers, A. P. (2020). The Natural Historian's Guide to the CT Galaxy: Step-by-Step Instructions for Preparing and Analyzing Computed Tomographic (CT) Data Using Cross-Platform, Open Access Software. *Integrative Organismal Biology*, *2*(1), obaa009. https://doi.org/10.1093/iob/obaa009

Chan, B. K. K., Chan, K. K. Y., & Leung, P. C. M. (2006). Burrow Architecture of the Ghost Crab Ocypode ceratophthalma on a Sandy Shore in Hong Kong. *Hydrobiologia*, *560*(1), 43–49. https://doi.org/10.1007/s10750-005-1088-2

Currey, J. D. (1984). *The mechanical adaptations of bones*. Princeton University Press.

De Schepper, N., De Kegel, B., & Adriaens, D. (2007). *Pisodonophis boro* (ophichthidae: Anguilliformes): Specialization for head‐first and tail‐first burrowing? *Journal of Morphology*, *268*(2), 112–126. https://doi.org/10.1002/jmor.10507

Dorgan, K. M. (2015). The biomechanics of burrowing and boring. *Journal of Experimental Biology*, *218*(2), 176–183. https://doi.org/10.1242/jeb.086983

Dorgan, K. M., Jumars, P. A., Johnson, B. D., & Boudreau, B. P. (2006). Macrofaunal burrowing: The medium is the message. *Oceanography and Marine Biology: An Annual Review*, *44*, 85–121.

https://www.researchgate.net/publication/228869644_Macrofaunal_burrowing_The_medium_is_the_message

Galbusera, F., & Bassani, T. (2019). The Spine: A Strong, Stable, and Flexible Structure with Biomimetics Potential. *Biomimetics*, *4*(3), 60. https://doi.org/10.3390/biomimetics4030060

Gambaryan, P. P., Gasc, J.-P., & Renous, S. (2003). Cinefluorographical study of the burrowing movements in the common mole, Talpa europaea (Lipotyphla, Talpidae). *Russian Journal of Theriology*, *1*(2), 91–109. https://doi.org/10.15298/rusjtheriol.01.2.03

Gerringer, M. E., Dias, A. S., Von Hagel, A. A., Orr, J. W., Summers, A. P., & Farina, S. (2021). Habitat influences skeletal morphology and density in the snailfishes (family Liparidae). *Frontiers in Zoology*, *18*(1), 16. https://doi.org/10.1186/s12983-021-00399-9

Gidmark, N. J., Strother, J. A., Horton, J. M., Summers, A. P., & Brainerd, E. L. (2011). Locomotory transition from water to sand and its effects on undulatory kinematics in sand lances (Ammodytidae). *Journal of Experimental Biology*, *214*(4), 657–664. https://doi.org/10.1242/jeb.047068

Haynes, T. B., Ronconi, R. A., & Burger, A. E. (2007). HABITAT USE AND BEHAVIOR OF THE PACIFIC SAND LANCE (AMMODYTES HEXAPTERUS) IN THE SHALLOW SUBTIDAL REGION OF SOUTHWESTERN VANCOUVER ISLAND. *Northwestern Naturalist*, *88*(3), 155–167.

https://doi.org/10.1898/1051-1733(2007)88%255B155:HUABOT%255D2.0.CO;2

Herrel, A., Choi, H. F., Dumont, E., De Schepper, N., Vanhooydonck, B., Aerts, P., & Adriaens, D. (2011). Burrowing and subsurface locomotion in anguilliform fish: Behavioral specializations and mechanical constraints. *Journal of Experimental Biology*, *214*(8), 1379–1385. https://doi.org/10.1242/jeb.051185

John Donald, C. (1984). Effects of differences in mineralization on the mechanical properties of bone. *Philosophical Transactions of the Royal Society of London. B, Biological Sciences*, *304*(1121), 509–518. https://doi.org/10.1098/rstb.1984.0042

Kassambara A (2023). *ggpubr: 'ggplot2' Based Publication Ready Plots*. R package version 0.6.0, <https://CRAN.R-project.org/package=ggpubr>

Long, J. H., Krenitsky, N. M., Roberts, S. F., Hirokawa, J., De Leeuw, J., & Porter, M. E. (2011). Testing Biomimetic Structures in Bioinspired Robots: How Vertebrae Control the Stiffness of the Body and the Behavior of Fish-Like Swimmers. *Integrative and Comparative Biology*, *51*(1), 158–175. https://doi.org/10.1093/icb/icr020

Monteleone, D. M., & Peterson, W. T. (1986). Feeding ecology of American sand lance Ammodytes americanus larvae from Long Island Sound. *Marine Ecology Progress Series*, *30*(2/3), 133–143. https://www.jstor.org/stable/24817546

Neuwirth E (2022). *RColorBrewer: ColorBrewer Palettes*. R package version 1.1-3, <https://CRAN.R-project.org/package=RColorBrewer>

Rolfe, S., Pieper, S., Porto, A., Diamond, K., Winchester, J., Shan, S., Kirveslahti, H., Boyer, D., Summers, A., & Maga, A. M. (2021). SlicerMorph: An open and extensible platform to retrieve, visualize and analyse 3D morphology. *Methods in Ecology and Evolution*, *12*(10), 1816–1825. https://doi.org/10.1111/2041-210X.13669

Shelton, R. M., Thornycroft, P., & Lauder, G. V. (2014). Undulatory locomotion of flexible foils as biomimetic models for understanding fish propulsion. *Journal of Experimental Biology*, jeb.098046. https://doi.org/10.1242/jeb.098046

Slice, D. E. (2007). Geometric Morphometrics. *Annual Review of Anthropology*, *36*(1), 261–281. https://doi.org/10.1146/annurev.anthro.34.081804.120613

Staudinger, M. D., Goyert, H., Suca, J. J., Coleman, K., Welch, L., Llopiz, J. K., Wiley, D., Altman, I., Applegate, A., Auster, P., Baumann, H., Beaty, J., Boelke, D., Kaufman, L., Loring, P., Moxley, J., Paton, S., Powers, K., Richardson, D., … Steinmetz, H. (2020). The role of sand lances (*Ammodytes* sp.) in the Northwest Atlantic Ecosystem: A synthesis of current knowledge with implications for conservation and management. *Fish and Fisheries*, *21*(3), 522–556. https://doi.org/10.1111/faf.12445

Tatom‐Naecker, T. M., & Westneat, M. W. (2018). Burrowing fishes: Kinematics, morphology and phylogeny of sand‐diving wrasses (Labridae). *Journal of Fish Biology*, *93*(5), 860–873. https://doi.org/10.1111/jfb.13789

Trueman, E. R. (1966). Bivalve Mollusks: Fluid Dynamics of Burrowing. *Science*, *152*(3721), 523–525. https://doi.org/10.1126/science.152.3721.523

Westneat, M. W., & Wainwright, S. A. (2001). 7. Mechanical design for swimming: Muscle, tendon, and bone. In *Fish Physiology* (Vol. 19, pp. 271–311). Elsevier. https://doi.org/10.1016/S1546-5098(01)19008-4

Wickham H, François R, Henry L, Müller K, Vaughan D (2023). *dplyr: A Grammar of Data Manipulation*. R package version 1.1.4, <https://CRAN.R-project.org/package=dplyr>

Wickham H (2023). *stringr: Simple, Consistent Wrappers for Common String Operations*. R package version 1.5.1, <https://CRAN.R-project.org/package=stringr>

Wickham H, Bryan J (2023). *readxl: Read Excel Files*. R package version 1.4.3, <https://CRAN.R-project.org/package=readxl>.

Wilke C (2024). *cowplot: Streamlined Plot Theme and Plot Annotations for 'ggplot2'*. R package version 1.1.3, <https://CRAN.R-project.org/package=cowplot>

Woodruff, E. C., Huie, J. M., Summers, A. P., & Cohen, K. E. (2022). Pacific Spiny Lumpsucker armor—Development, damage, and defense in the intertidal. *Journal of Morphology*, *283*(2), 164–173. https://doi.org/10.1002/jmor.21435

Acknowledgements

The authors would like to acknowledge that this research was supported by funding from the Mary Gates Endowment for Students and Friday Harbor Laboratories.